Molecular Biology of the Cell
Vol. 10, 1957–1972, June 1999

Vesicle-associated Membrane Protein 4 is Implicated in *Trans*-Golgi Network Vesicle Trafficking

Martin Steegmaier,* Judith Klumperman,† Davide L. Foletti,* Jin-San Yoo,* and Richard H. Scheller*‡

*Department of Molecular and Cellular Physiology, Howard Hughes Medical Institute, Stanford University School of Medicine, Stanford, California 94305-5345; and †Department of Cell Biology, School of Medicine, Research Institute for Biomembranes, University of Utrecht, 3584CX Utrecht, The Netherlands

Submitted December 28, 1998; Accepted March 23, 1999
Monitoring Editor: Randy W. Schekman

The *trans*-Golgi network (TGN) plays a pivotal role in directing proteins in the secretory pathway to the appropriate cellular destination. VAMP4, a recently discovered member of the vesicle-associated membrane protein (VAMP) family of trafficking proteins, has been suggested to play a role in mediating TGN trafficking. To better understand the function of VAMP4, we examined its precise subcellular distribution. Indirect immunofluorescence and electron microscopy revealed that the majority of VAMP4 localized to tubular and vesicular membranes of the TGN, which were in part coated with clathrin. In these compartments, VAMP4 was found to colocalize with the putative TGN-trafficking protein syntaxin 6. Additional labeling was also present on clathrin-coated and noncoated vesicles, on endosomes and the medial and *trans* side of the Golgi complex, as well as on immature secretory granules in PC12 cells. Immunoprecipitation of VAMP4 from rat brain detergent extracts revealed that VAMP4 exists in a complex containing syntaxin 6. Converging lines of evidence implicate a role for VAMP4 in TGN-to-endosome transport.

INTRODUCTION

Secretory pathway compartments can be subdivided into two central membrane populations, the endoplasmic reticulum (ER)–Golgi system and the *trans*-Golgi network (TGN)–endosomal system. The ER–Golgi system performs the folding, oligomerization, and co- and post-translational modifications of proteins transiting the secretory pathway. The TGN–endosomal system is central to the sorting, export, and recycling of numerous soluble and membrane-associated lysosomal and secretory pathway proteins. At the TGN, newly synthesized proteins are routed to endosomes and lysosomes, to regulated and constitutive exocytic pathways, and, in polarized cells, to apical and basolateral membranes (Palade, 1975; Mellman and Simons, 1992; Rothman and Wieland, 1996; Schekman and Orci, 1996; Traub and Kornfeld, 1997). The TGN also receives membrane traffic from the endocytic pathway; e.g., the two mannose 6-phosphate receptors (MPRs) carry lysosomal hydrolases from the TGN to late endosomes, where they release the hydrolases and then return to the TGN for another round of transport (Kornfeld, 1992). Movement of protein between these compartments occurs by the budding and fusion of transport vesicles. Maintaining the identity of membrane-bound compartments in the face of the massive flux between them requires the orchestrated interaction of a large number of components, including lipid, cytosolic proteins such as ATPases and GTPases and integral membrane proteins present on target membranes and transport vesicles.

The most intensely studied vesicle and target membrane proteins are members of the vesicle-associated membrane protein (VAMP)/synaptobrevin, syntaxin, and synaptosomal-associated protein of 25 kDa (SNAP-25) families. These proteins, also known as soluble *N*-ethylmaleimide–sensitive factor (NSF) at-

‡ Corresponding author. E-mail address: scheller@cmgm.stanford.edu.

© 1999 by The American Society for Cell Biology

tachment protein (SNAP) receptors or SNAREs, have been implicated to be, at least in part, necessary in determining the specificity of vesicle transport. Vesicle and target membrane SNAREs form tight oligomeric protein complexes proposed to direct membrane fusion (Sollner *et al.*, 1993b; Bennett and Scheller, 1994; Hanson *et al.*, 1997b; Hay and Scheller, 1997; Weber *et al.*, 1998). One of the best studied trafficking pathways occurs at the synapse, where neurotransmitter-filled synaptic vesicles undergo local exocytic and endocytic cycles to mediate neuronal communication (Scheller, 1995; Sudhof, 1995; Hanson *et al.*, 1997a). The interaction of the synaptic vesicle SNARE (v-SNARE) VAMP/synaptobrevin with the target SNAREs (t-SNAREs) syntaxin 1a and SNAP-25 results in the formation of an SDS-resistant complex that migrates at 7S in density gradients (Sollner *et al.*, 1993a). The 7S core complex is formed by four α-helices, two of them contributed by SNAP-25 and one each from syntaxin and VAMP (Poirier *et al.*, 1998). At the center of the 7S structure is an ionic layer consisting of an arginine residue and three glutamate residues contributed from each of the four α-helices (Sutton *et al.*, 1998). These residues are highly conserved across the entire SNARE family. Members of the VAMP/synaptobrevin family contain a conserved arginine residue and are therefore also called R-SNAREs. Syntaxin family members contain a conserved glutamine in the center of their carboxyl-terminal helical domain and SNAP-25 related SNAREs have a conserved glutamine in each of their two helical domains. Therefore, these vesicle-trafficking molecules are also called Q-SNAREs.

Recently, several SNARE proteins have been characterized based on interactions with known SNAREs or by sequence homology to known SNARE proteins (McMahon *et al.*, 1993; Bock *et al.*, 1996; Hay *et al.*, 1996; Advani *et al.*, 1998; Steegmaier *et al.*, 1998; Zeng *et al.*, 1998). In mammalian species, there are now ~10 R-SNAREs identified, which localize to different subcellular compartments. VAMP/synaptobrevin 1 and 2 are highly homologous (~80% amino acid identity) membrane proteins associated with synaptic vesicles and secretory granules (SGs), whereas VAMP3/cellubrevin is ubiquitously expressed and is associated with the endocytic pathway (McMahon *et al.*, 1993; Galli *et al.*, 1994). VAMP4 was broadly expressed and localized to the Golgi–TGN when an epitope-tagged version of this protein was transfected into normal rat kidney (NRK) cells (Advani *et al.*, 1998). Zeng *et al.* (1998) reported that another VAMP homologous protein (VAMP5) is increased during in vitro myogenesis in which it is present on the plasma membrane. VAMP7 and VAMP8 localize to late and early endosomes, respectively (Advani *et al.*, 1998; Wong *et al.*, 1998). The VAMP homologue rsec22b localizes to ER and intermediate compartment and forms a stable complex with syntaxin 5, membrin, and rbet1 (Hay *et al.*, 1997, 1998). ERS-24, a mammalian R-SNARE homologous to yeast sec22p and mammalian rsec22b, has also been implicated in vesicle trafficking between the ER and the Golgi, although formal proof for the function of ERS-24 has yet to be determined (Paek *et al.*, 1997). Yet another R-SNARE has been implicated in ER-to-Golgi transport. Ykt6p and its homologues are highly conserved from yeast to human, as demonstrated by the functional complementation of the loss of Ykt6p by its human counterpart (McNew *et al.*, 1997).

To better understand vesicle flow patterns within mammalian cells, it is clearly of interest to isolate and characterize new SNARE proteins. In this report, we define the precise subcellular distribution of VAMP4. Indirect immunofluorescence and electron microscopy revealed that VAMP4 localizes to tubovesicular membranes of the TGN, which were in part coated with clathrin. VAMP4 was found to colocalize with syntaxin 6 in these compartments. Furthermore, we show that VAMP4 exists in a syntaxin 6–containing SNARE complex. Our data indicate a role for VAMP4 in TGN-to-endosome transport.

MATERIALS AND METHODS

Antibodies

A rabbit antiserum against VAMP4 was raised by subcutaneous injection of a bacterially expressed full-length cytoplasmic domain of VAMP4. The expression construct included amino acids 2–115 of human VAMP4 fused to GST. For affinity purification, the antiserum was first incubated with cyanogen bromide (CNBr)–activated Sepharose beads (Sigma, St. Louis, MO) coupled with GST. The flow through was then incubated with thrombin-cleaved recombinant VAMP4 coupled to CNBr-activated Sepharose beads (2 mg protein/ml beads). The VAMP4-CNBr Sepharose beads were washed extensively, and bound antibodies were eluted using 0.1 M glycine, pH 2.8. Eluates containing the affinity-purified antibodies were neutralized and stored at 4°C in the presence of 0.02% sodium azide. Anti-syntaxin 6 monoclonal (clone 3D10), anti-syntaxin 1A monoclonal (HPC-1), anti-p115 monoclonal, and anti-VAMP2 polyclonal antibodies were described previously (Inoue *et al.*, 1992; Waters *et al.*, 1992; Pevsner *et al.*, 1994; Bock *et al.*, 1997). Mouse anti-transferrin receptor antibodies were purchased from Zymed Laboratories (South San Francisco, CA). Mouse monoclonal anti-synaptophysin antibody was obtained from Boehringer Mannheim (Mannheim, Germany). Mouse monoclonal anti-clathrin (C43820) antibody was purchased from Transduction Laboratories (Lexington, KY). Texas Red–labeled anti-rabbit immunoglobulin G (IgG) and FITC-labeled anti-mouse IgG secondary antibodies were obtained from Jackson ImmunoResearch (West Grove, PA). Rabbit anti-rbet1 has been described previously (Hay *et al.*, 1998), and rabbit-anti mouse IgG antibody was purchased from Dako (Glostrup, Denmark). As a control antibody for the double-immunogold labeling procedure, we used mouse mAb 3C9.H6 (Zen *et al.*, 1998), which was raised against lamellar bodies of alveolar type II cells and gives no immunostaining in PC12 cells.

Indirect Immunofluorescence Microscopy

Cell lines were maintained in a 5% CO_2 incubator using routine media formulations. Before fixation, PC12 cells were differentiated for 4 d in the presence of 15 ng/ml nerve growth factor (Life

Technologies, Gaithersburg, MD). Primary hippocampal CA3/CA1 embryonic cultures were obtained and maintained as described previously (Banker and Cowan, 1977). For drug treatments before immunofluorescence microscopy, Chinese hamster ovary (CHO) cells were incubated for 15 min with growth medium containing 10 μg/ml brefeldin A (BFA; Calbiochem, San Diego, CA) or for 30 min with 5 μg/ml nocodazole (Calbiochem). Cells were then fixed and processed for indirect immunofluorescence microscopy as described previously (Hay *et al.*, 1996).

Immunogold Labeling of Ultrathin Cryosections

Nondifferentiated PC12 cells were fixed for 2 h at room temperature in a mixture of 2% freshly prepared formaldehyde and 0.2% glutaraldehyde in 0.1 M sodium phosphate buffer, pH 7.4. Fixed cells were embedded in 10% gelatin and, after 4 h penetration with 2.3 M sucrose at 4°C, quickly frozen in liquid nitrogen. Ultrathin cryosectioning was performed using the improved pickup method with a mixture of sucrose and methylcellulose (Liou *et al.*, 1996), and subsequent double-immunogold labeling was carried out according to the protocol previously described by Slot *et al.* (1991). Antibodies were visualized for electron microscopy by incubation with protein A conjugated to 10- or 15-nm gold particles (protein A-gold). Because protein A on sections only poorly binds to mouse antibodies, an extra labeling step with rabbit anti-mouse IgG was performed when the primary antibody was derived from mouse (i.e., in the case of clathrin and 3C9.H6). To establish the relative distribution pattern of VAMP4, sections were double labeled with anti-VAMP4/protein A-15-nm gold in the first step and anti-clathrin/rabbit anti-mouse IgG/protein A-10-nm gold in the second step. In the electron microscope, areas of the grid were selected that exhibited optimal preserved ultrastructure, and at a magnification of 25,000× all VAMP4-representing gold particles within a distance of 30 nm from a membrane were counted and ascribed to the compartment over which they were located. The presence of clathrin on a VAMP4-positive membrane was judged by the occurrence of 10-nm gold labeling. We used anti-VAMP4 in the first step because the immunogold staining obtained for clathrin is rather dense and when applied in the first step might sterically hinder anti-VAMP4 antibodies to label clathrin-coated vesicles. Between the two labeling steps, sections were fixed with 1% glutaraldehyde, which destroys the binding sites for protein A on the first primary antibody (Slot *et al.*, 1991). As a control for this labeling procedure we performed a double labeling in which anti-VAMP4/protein A-10-nm gold staining was followed by a control antibody (mouse mAb 3C9.H6 and rabbit anti-mouse IgG) and protein A-15-nm gold. In this staining, only VAMP4-representing 10-nm gold particles were found (see Figure 6A). A similar result was obtained when the second primary antibody was omitted. This control proves the specificity of the double-labeling procedure and indicates that colocalization of VAMP4 with clathrin and syntaxin 6 is not a result of nonspecific binding of the second protein A-gold to the VAMP4 antibody. To distinguish between distinct intracellular compartments the following criteria were used. In PC12 cells, the TGN at the *trans* side of the Golgi can easily be distinguished from the *cis*-Golgi–located ER–Golgi intermediate compartment by the presence of immature SGs (ISGs) and clathrin-coated vesicles and tubules. In our quantitation we considered all membranes that were found in close vicinity with and at the *trans* side of a Golgi stack as TGN. ISGs, many of which were located in the TGN area, were assigned as a separate category, because their rounded shape and dense protein content allowed us to unequivocally discriminate them from other membranes in the TGN area. ISGs were distinguished from mature SGs by the presence of a clathrin coat (Orci *et al.*, 1985; Tooze and Tooze, 1986; Klumperman *et al.*, 1998). The Golgi stack itself was recognized by its characteristic morphology of non–clathrin-coated, stacked cisternae. A small percentage of VAMP4 staining was found over vesicles that at least in the plane of the section were not seen in close association with the Golgi stack. Although these vesicles could well be part of the TGN, in ultrathin sections the Golgi stack is not always visible in the plane of the section; they did not meet our criteria and were therefore denoted cytosolic. In total, 482 gold particles were counted in four independent counting sessions on two different electron microscopy grids. Finally, the percentage of the total gold particles that was found over a specific compartment was calculated (see Table 1).

Glycerol Velocity Gradients

Freshly isolated rat brain was homogenized in 20 mM HEPES, pH 7.4, 10 mM sucrose, 120 mM KCl, 2 mM EDTA, 2 mM EGTA, 6 mM $MgCl_2$, 1 mM DTT, 0.3 mM PMSF, 2 μg/ml leupeptin, 4 μg/ml aprotinin, and 0.7 μg/ml pepstatin using a glass-Teflon homogenizer. The homogenate was centrifuged at 1000 × *g* for 15 min, and the resulting supernatant (postnuclear supernatant) was centrifuged at 100,000 × *g* for 1 h. The resulting pellet was resuspended in 20 mM HEPES, pH 7.4, 100 mM KCl, 2 mM EDTA, 2 mM EGTA, 1 mM DTT, plus the above-mentioned protease inhibitors. Membranes were then extracted with 1% Triton X-100 for 30 min, and insoluble material was sedimented at 100,000 × *g* for 1 h. Glycerol gradients (11–35%) were prepared as described previously (Hay *et al.*, 1997). After centrifugation sequential fractions were resolved on 14% SDS-polyacrylamide gels, immunoblotted, and probed for the presence of VAMP4, VAMP2, syntaxin 6, syntaxin 1, and synaptophysin.

Immunoprecipitation Experiments and Protein Sequencing

Affinity-purified anti-VAMP4 antibodies and control rabbit antibodies were bound to protein A-Sepharose beads (Amersham Pharmacia Biotech, Arlington Heights, IL) and cross-linked with dimethylpimedilate (Sigma). Frozen brains from Sprague Dawley rats were homogenized in 50 mM Tris-HCl, pH 8.0, 150 mM NaCl, 1 mM EDTA, 1 mM EGTA, 1 mM DTT, plus the above-mentioned protease inhibitors (homogenization buffer). The homogenate was centrifuged at 1000 × *g* for 10 min to obtain postnuclear supernatant. A final 100,000 × *g* centrifugation was performed, the supernatant was discarded, and the pellet was resuspended in homogenization buffer. This fraction was then extracted with 1% Triton X-100 for 1 h, followed by centrifugation at 100,000 × *g* for 30 min. The supernatant containing ~20 mg/ml protein was preadsorbed with protein A-Sepharose for 3 h. Preadsorbed rat brain membrane lysates were then mixed with antibody beads with agitation for 10–12 h at 4°C. After the binding step, the antibody beads were washed four times with immunoprecipitation wash buffer I (50 mM Tris-HCl, pH 8.0, 250 mM NaCl, 0.1% Triton X-100, and 1 mg/ml BSA) and two times with immunoprecipitation wash buffer II (50 mM Tris-HCl, pH 8.0, and 250 mM NaCl). The bound material was eluted off the antibody beads by incubating them for 30 min at 50°C with SDS sample buffer without reducing agent. The eluted proteins were then separated on a 14% SDS-polyacrylamide gel and stained with Coomassie blue. Individual protein bands were cut out and subjected to in-gel proteolysis by lysC. The digested peptides were fractionated by HPLC and microsequenced as described previously (Hsu *et al.*, 1996). In addition, some peptide mixtures were subjected to mass spectrometric analysis. For small-scale immunoprecipitation experiments (e.g., Figure 9B), protein A-Sepharose and 5 μg of control antibodies, anti-VAMP4 polyclonal antibodies, or anti-syntaxin 6 antibody (clone 3D10) were added to equal aliquots of preadsorbed rat brain membrane lysates and incubated for 12 h at 4°C. The antibody beads were then washed and eluted as described above. Equal aliquots of the eluates were resolved on 14% SDS-polyacrylamide gels, immunoblotted, and probed for the presence of VAMP4, syntaxin 6, and synaptophysin.

RESULTS

VAMP4 Is Broadly Expressed

To corroborate our previously determined VAMP4 transcript distribution (Advani *et al.*, 1998), we performed Western blot analysis using affinity-purified antibodies prepared by immunizing rabbits with recombinant VAMP4 protein. These antibodies recognized a single band of 18 kDa in rat brain postnuclear supernatant. This band was eliminated by preincubating the antibodies with soluble recombinant VAMP4 but not with recombinant VAMP1 or 2 (Figure 1A). VAMP4 was found to be broadly expressed, with highest expression levels in brain and testis (Figure 1B). This broad tissue distribution was also reflected by the high expression level of VAMP4 observed in various cell lines derived from five different species (Figure 1C). VAMP4 seemed to be particularly enriched in PC12 cells. In some cases, a less prominent band at ~14 kDa could also be detected (Figure 1, B and C). This band most likely represents a degradation product of VAMP4, because the use of slowly processed tissue samples or cell line lysates for Western blot analysis resulted in an increased level of this lower-molecular-mass band. In liver lysates a prominent band of 25 kDa was detected (Figure 1B). It is possible that this 25-kDa band represents the product of an alternatively spliced VAMP4 transcript, because Northern blot analysis revealed the presence of multiple VAMP4 transcripts (Advani *et al.*, 1998). The broad tissue expression indicates that VAMP4 is involved in a constitutive vesicle-trafficking step common to most cell types.

VAMP4 Colocalizes with Syntaxin 6 in the TGN

We had shown previously that epitope-tagged VAMP4 localized to a juxtanuclear region in NRK cells much like the *trans*-Golgi network SNARE syntaxin 6 (Bock *et al.*, 1997; Advani *et al.*, 1998). To determine the subcellular localization of endogenous VAMP4, we stained NRK, COS-7, nerve growth factor–differentiated PC12 cells, and hippocampal neurons with the affinity-purified polyclonal anti-VAMP4 antibodies. In all these cells, the immunoreactivity was localized in a juxtanuclear area, again consistent with our previous study (Figure 2). Interestingly, in nerve growth factor–differentiated PC12 cells as well as in embryonic hippocampal cultures, the staining was strictly localized to the juxtanuclear region. No detectable immunoreactivity was observed in dendritic or axonal processes (Figure 2, C and D). In contrast, indirect immunofluorescence studies with antibodies against VAMP2 showed a high level of immunoreactivity in the processes as well as in the cell body.

To further understand the trafficking pathway in which VAMP4 functions, we performed colocalization studies with antibodies against different markers for TGN, *cis*-Golgi, and recycling and sorting endosomes. To this end, CHO cells were fixed, permeabilized, and stained with anti-VAMP4 antibodies (Figure 3, A, D, and G). As in NRK cells, the anti-VAMP4 staining observed in CHO cells was sometimes restricted to a defined juxtanuclear area, but more often perinuclear vesicular structures seemed to partially or entirely surround the nucleus (Figures 2A and 3, A, D, and G). The pattern of the VAMP4 staining almost completely overlapped with that of syntaxin 6 known to be enriched in the TGN (Figure 3, A–C). Costaining of VAMP4 and syntaxin 6 was also performed in NRK and PC12 cells, as well as in embryonic hippocampal cultures, and in all cases the two staining patterns overlapped strikingly. At this level of resolution significant overlap was also observed with p115, a peripheral membrane protein localized to the *cis*-Golgi, and originally identified as a component required for intra-Golgi transport (Figure 3E) (Waters *et al.*, 1992; Nakamura *et al.*, 1997). However, when anti-VAMP4 and anti-p115 stainings were merged, it became obvious that the two immunoreactivities were in close proximity but did not overlap completely (Figure 3F). In contrast, transferrin receptor, a well-established marker for recycling and sorting endosomes, showed only partial overlap with VAMP4 (Figure 3, G–I). Anti-transferrin receptor antibodies stained the peri-Golgi region, juxtaposed to the Golgi stacks, but unlike the VAMP4 staining the transferrin receptor immunoreactivity extended further into the periphery of the cells. Taken together, our colocalization studies indicate that VAMP4 is preferentially associated with membranes of the Golgi–TGN.

The dynamics of proteins in the presence of the fungal metabolite BFA and other membrane flow perturbants can reveal features of their native localization and life cycle (Klausner *et al.*, 1992). BFA causes a block in ER-to-Golgi membrane trafficking and induces Golgi proteins to return to the ER via a retrograde tubovesicular pathway (Lippincott-Schwartz *et al.*, 1990; Orci *et al.*, 1991). Furthermore, BFA also results in the tubulation of the endosomal system and the TGN, causing them to collapse around the microtubule-organizing center (MTOC) (Lippincott-Schwartz *et al.*, 1991; Reaves and Banting, 1992). Therefore, the perturbance of membrane flow with BFA can be used to determine whether a protein of interest is associated with the Golgi complex or with the TGN–endosomal system. Because Golgi versus TGN staining cannot be readily distinguished in unperturbed cells, we tested whether the treatment of CHO cells with BFA would cause VAMP4 to relocalize to the ER or to the MTOC. A 15-min treatment of CHO cells with 5 μg/ml BFA was sufficient to cause VAMP4 to almost entirely collapse around the MTOC (Figure 4, A, D, and G). Likewise, the TGN SNARE

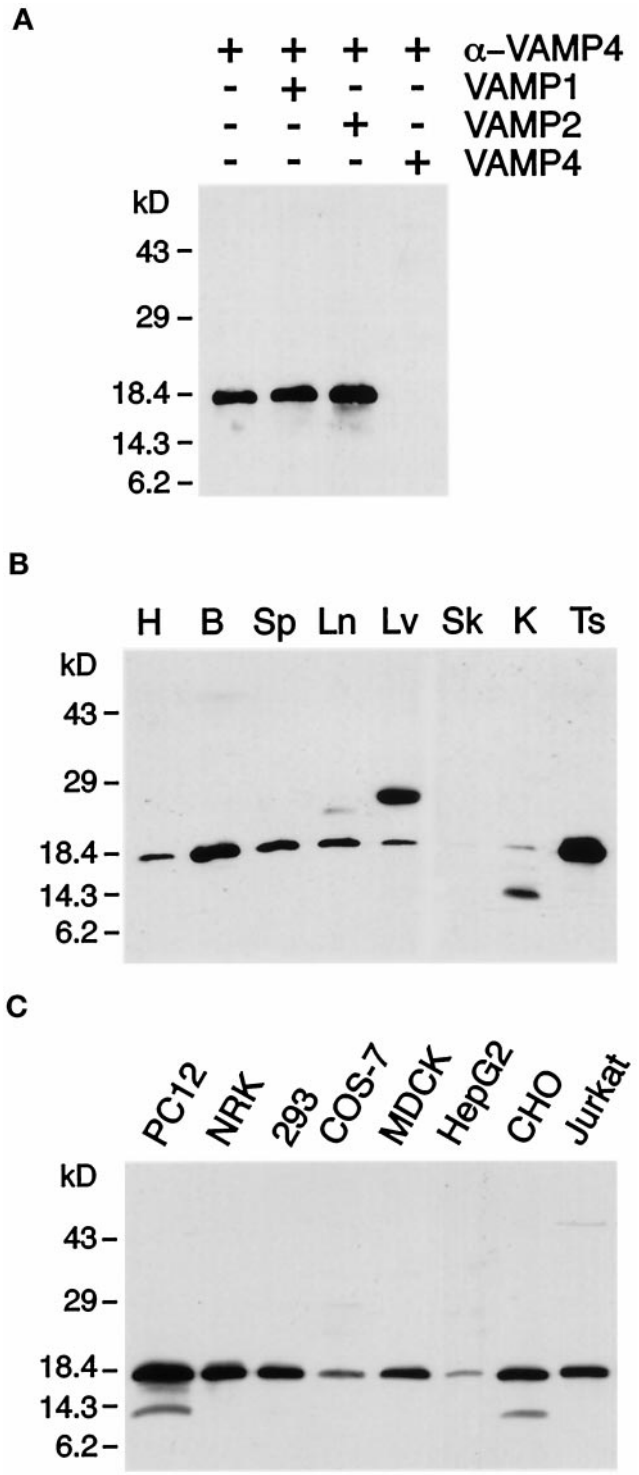

Figure 1. VAMP4 is broadly expressed. (A) Anti-VAMP4 antibodies preincubated with control buffer or recombinant VAMP1 or VAMP2 but not antibodies preincubated with recombinant VAMP4 recognize an 18-kDa band in brain postnuclear supernatant (PNS). (B) PNSs from rat heart (H), brain (B), spleen (Sp), lung (Ln), liver (Lv), skeletal muscle (Sk), kidney (K), and testis (Ts) (30 μg/lane) were analyzed by Western blot using affinity-purified rabbit polyclonal antibodies. A major band is detected at 18 kDa, with highest expression levels in brain and testis. The ~25-kDa band in liver is recognized by polyclonal antibodies purified from two different rabbits immunized with VAMP4, suggesting that two isoforms of VAMP4 are expressed in liver. The lower-molecular-mass band recognized by the anti-VAMP4 antibodies in kidney PNS represents a degradation product of VAMP4. (C) PNSs of various cell lines (30 μg/lane) were analyzed by Western blot using affinity-purified rabbit polyclonal antibodies. VAMP4 was detected in all cell lines examined. The lower-molecular-mass band recognized by the anti-VAMP4 antibodies in PC12 and CHO cell lysate represents a degradation product of VAMP4.

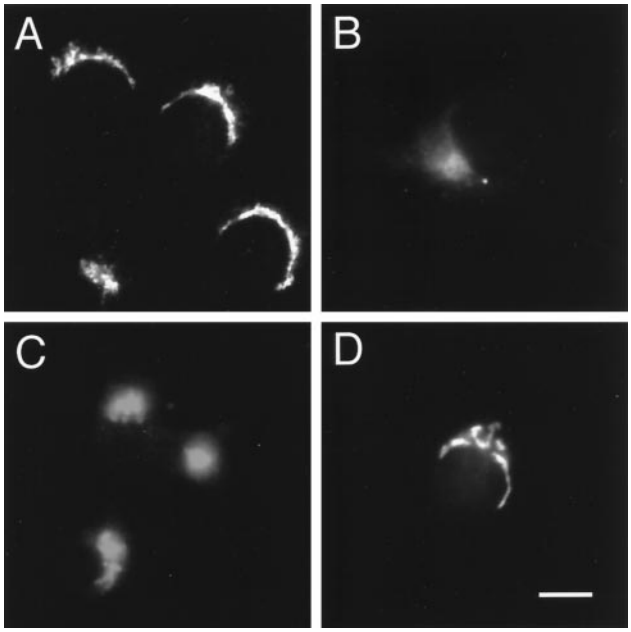

Figure 2. Perinuclear labeling for VAMP4 is detected in cell lines and primary cultures. Cells were fixed with 4% paraformaldehyde, permeabilized with saponin, and stained using affinity-purified anti-VAMP4 polyclonal antibodies and Texas Red–conjugated anti-rabbit IgG secondary antibody before processing for indirect immunofluorescence microscopy. (A) NRK; (B) COS-7; (C) NGF-differentiated PC12; (D) 12 d in vitro embryonic hippocampal cultures. Note that there is no VAMP4 staining observed in the processes of differentiated PC12 cells or embryonic hippocampal cultures. Bar: A–C, 20 μm; D, 25 μm.

syntaxin 6 collapsed to the identical region of the cell as VAMP4 (Figure 4, B and C). Incubation of CHO cells with BFA for an extended period did not result in a redistribution of either VAMP4 or syntaxin 6, compared with the localization observed after a 15-min BFA treatment. After a 2-h treatment with BFA, VAMP4 and syntaxin 6 remained colocalized in a compact spot in the center of the cell. As expected for proteins associated with the Golgi complex, p115 did not collapse into the MTOC. Unlike VAMP4, p115 was redistributed to spotty vesicular structures reminiscent of staining patterns observed for proteins associ-

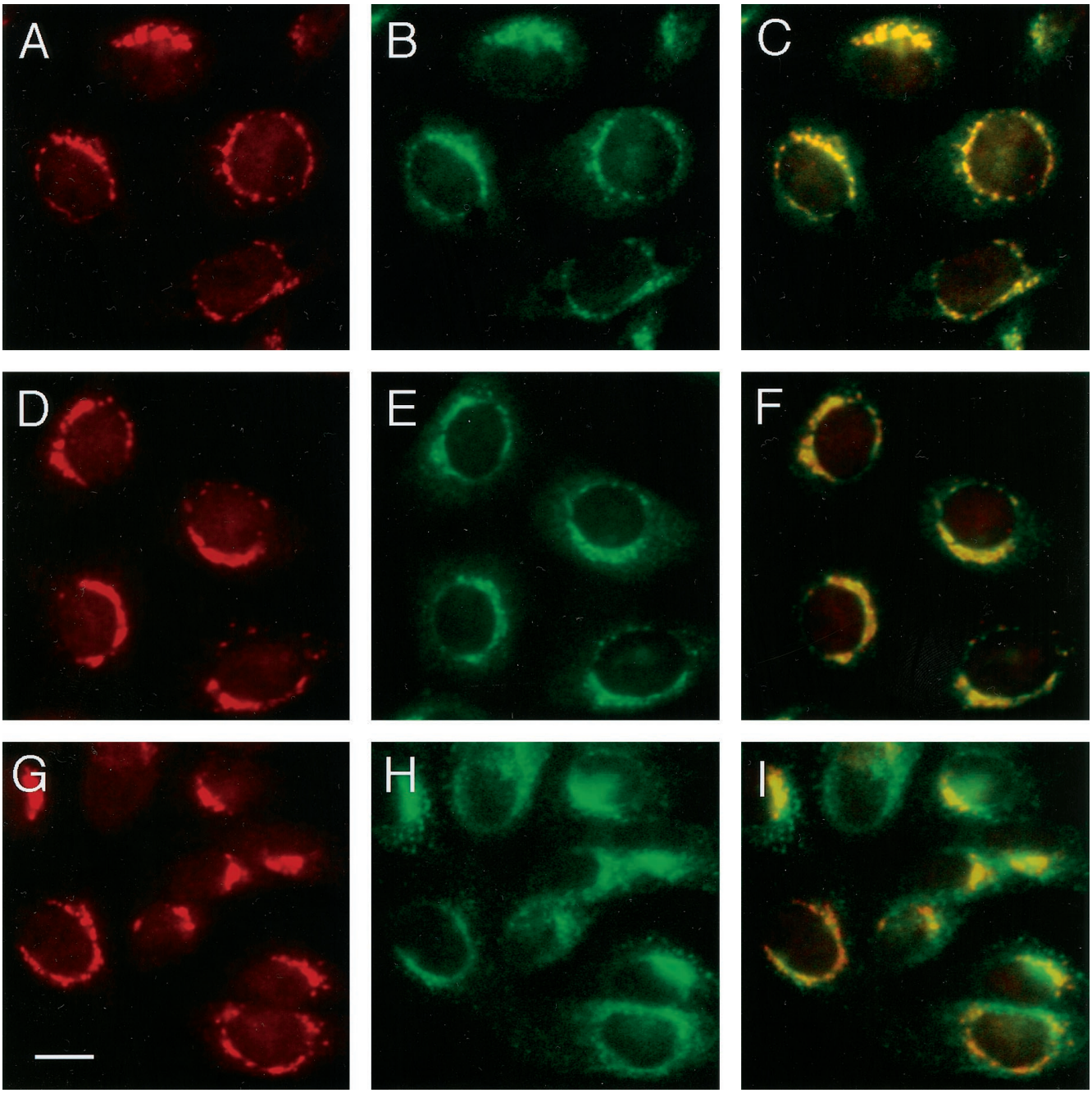

Figure 3. VAMP4 colocalizes with syntaxin 6. CHO cells were fixed with 4% paraformaldehyde, permeabilized with saponin, and costained using affinity-purified rabbit anti-VAMP4 antibodies (A, D, and G) and mouse mAbs against syntaxin 6 (B), p115 (E), and transferrin receptor (H). Texas Red–labeled anti-rabbit IgG and FITC-labeled anti-mouse IgG were used as secondary antibodies before processing for indirect immunofluorescence microscopy. In yellow are areas of overlap in merged images (C, F, and I). Bar, 20 μm.

ated with the intermediate compartment (Figure 4, D–F). Much like VAMP4 and syntaxin 6, transferrin receptor collapsed after 15 min of BFA treatment around the MTOC. Interestingly, after 15 min of BFA treatment VAMP4 and syntaxin 6 almost entirely relocalized to the MTOC, whereas a markable pool of the transferrin receptor was still associated with tubular structures around the MTOC (Figure 4, A–C vs. G–I). Our results indicate that during BFA treatment both vesicle-trafficking proteins, VAMP4 and syntaxin 6, follow a similar pathway taken by a marker of the endosomal compartment such as the transferrin recep-

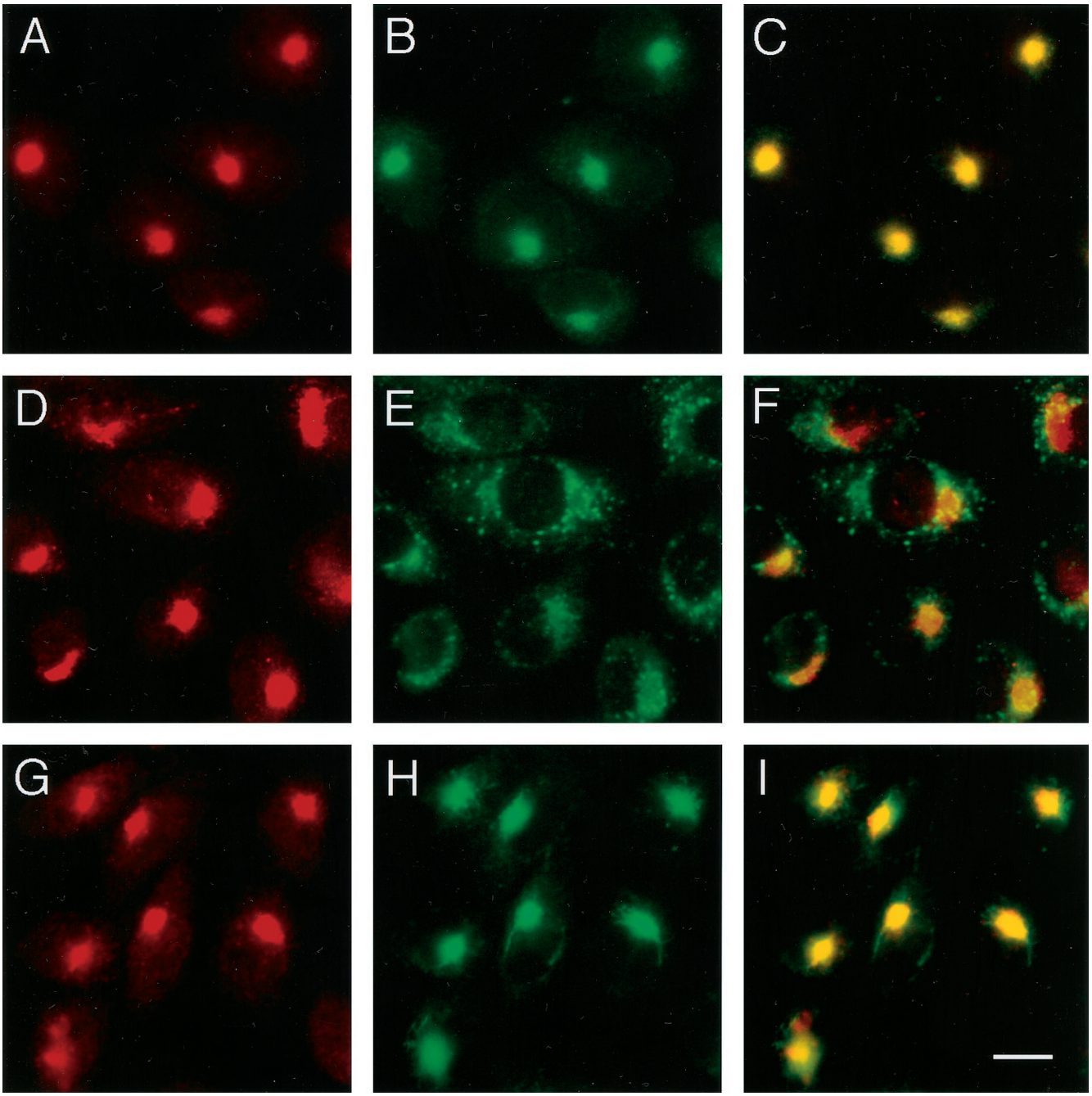

Figure 4. VAMP4 and syntaxin 6 both localize to the same compartment upon BFA treatment. CHO cells, treated for 15 min with 10 μg/ml BFA, were fixed with 4% paraformaldehyde, permeabilized with saponin, and costained using affinity-purified rabbit anti-VAMP4 antibodies (A, D, and G) and mouse mAbs against syntaxin 6 (B), p115 (E), and transferrin receptor (H). Texas Red–labeled anti-rabbit IgG and FITC-labeled anti-mouse IgG were used as secondary antibodies before processing for indirect immunofluorescence microscopy. In yellow are areas of overlap in merged images (C, F, and I). Bar, 20 μm.

tor. However, VAMP4 and syntaxin 6 do not precisely colocalize with transferrin receptor after 15 min of BFA treatment or in untreated cells.

To obtain additional evidence that the bulk of VAMP4 resides in the TGN but not within the endosomal compartment, we treated CHO cells for 30 min with the microtubule-depolymerizing drug nocodazole. Nocodazole-induced microtubule depolymerization causes the scattering and fragmentation of the Golgi complex and the TGN into cytoplasmic vesicu-

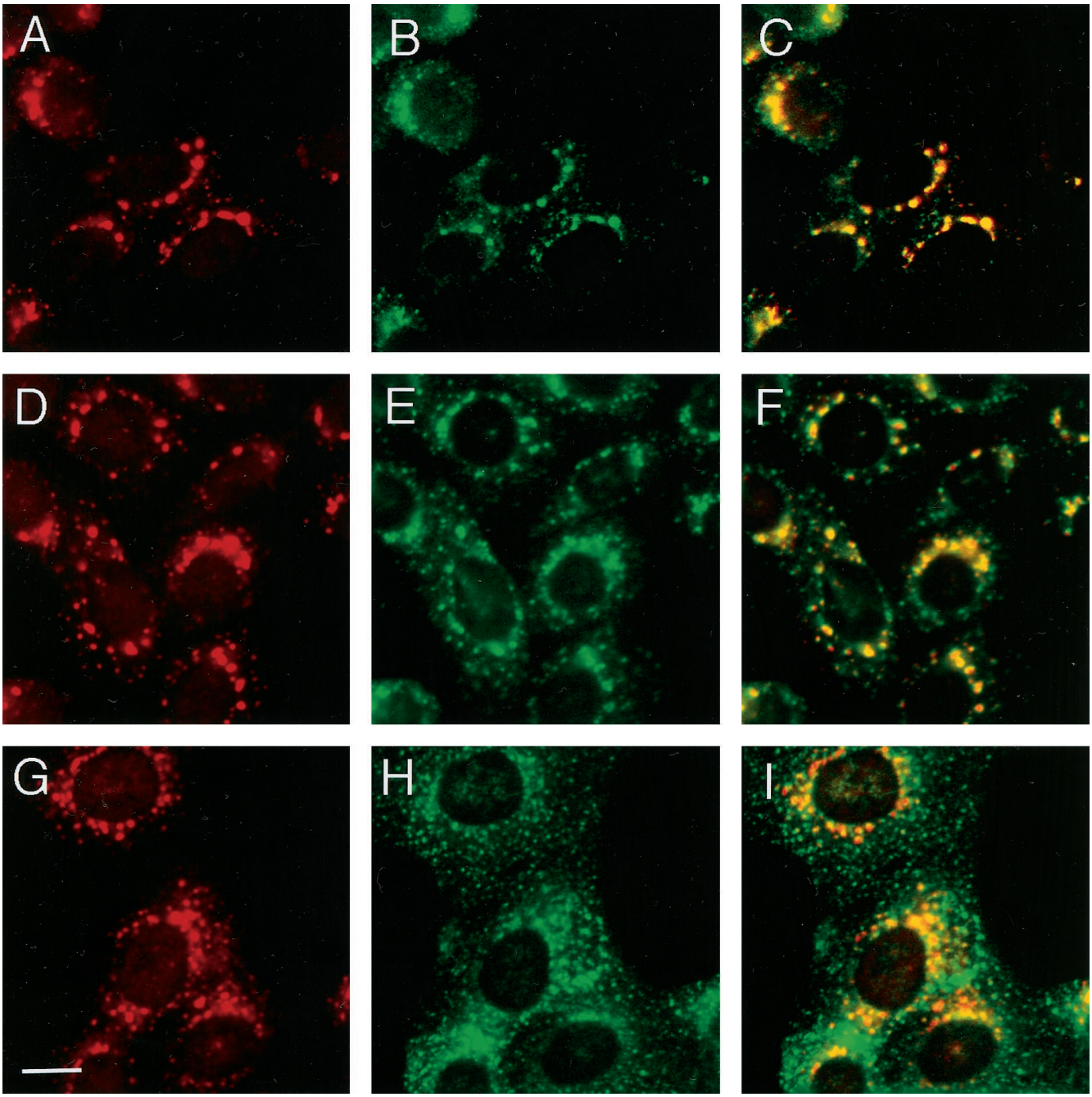

Figure 5. Nocodazole causes redistribution of VAMP4 and syntaxin 6 to the same compartment. CHO cells, treated for 30 min with 5 μg/ml nocodazole, were fixed with 4% paraformaldehyde, permeabilized with saponin, and costained using affinity-purified rabbit anti-VAMP4 antibodies (A, D, and G) and mouse mAbs against syntaxin 6 (B), p115 (E), and transferrin receptor (H). Texas Red-labeled anti-rabbit IgG and FITC-labeled anti-mouse IgG were used as secondary antibodies before processing for indirect immunofluorescence microscopy. In yellow are areas of overlap in merged images (C, F, and I). Bar, 20 μm.

lar structures (Turner and Tartakoff, 1989; Reaves and Banting, 1992). An intact microtubule network is also necessary for the integrity of the endosomal system (Matteoni and Kreis, 1987). Upon nocodazole treatment, transferrin is dispersed into numerous regularly shaped structures, which scatter uniformly throughout the cytoplasm (Lippincott-Schwartz *et al.*, 1991). Treatment of CHO cells with nocodazole caused VAMP4 immunoreactivity to fragment into vesicular structures surrounding the nuclear envelope and ex-

Table 1. Relative distribution of VAMP4 in PC12 cells

	Percentage of total gold particles ± SD
Golgi stack	21.5 ± 6.1
TGN total	51.8 ± 2.5
Clathrin-coated	21.8 ± 2.8
Non–clathrin-coated	33.8 ± 4.6
Clathrin-coated vesicles	8.5 ± 2.6
Noncoated vesicles	4.3 ± 2.6
Endosomes	6.3 ± 3.6
ISGs	6.8 ± 3.8

Quantifications were carried out in two different electron microscopic grids, on sections double-immunogold labeled for VAMP4 and clathrin.

tending into the cytoplasm (Figure 5, A, D, and G). Most of these VAMP4-containing vesicular structures contained syntaxin 6 (Figure 5, A and B), indicating that the majority of the VAMP4 and syntaxin 6 immunoreactivity resides within the TGN. Similarly, upon nocodazole treatment the p115 staining dispersed into vesicular structures (Figure 5E). Although a significant pool of these structures colocalized with the VAMP4 immunoreactivity, many p115-containing vesicular structures were completely devoid of VAMP4 (Figure 5F). Labeling of nocodazole-treated CHO cells with anti-transferrin receptor antibodies resulted in a staining pattern clearly distinct from that for VAMP4 (Figure 5, G–I). Anti-transferrin receptor antibodies labeled uniformly distributed vesicular structures, which are smaller in size, greater in number, and clearly distinguishable from the vesicular structures stained with anti-VAMP4 antibodies. Taken together, the costaining experiments and the treatment of cells with BFA and nocodazole firmly established that VAMP4, like syntaxin 6, is preferentially associated with the TGN.

VAMP4 Is Localized to the Trans-Golgi and Clathrin-coated and Non–Clathrin-coated Membranes of the TGN

To assess the localization of VAMP4 at the ultrastructural level, ultrathin cryosections of PC12 cells were immunogold labeled for VAMP4. The labeling obtained for VAMP4 was specific (nonspecific staining over the nucleus was virtually absent; see Figure 7B) and highly reproducible (Table 1). Approximately 75% of total VAMP4 gold particles were found over the Golgi stack and TGN (Table 1 and Figure 6A), and a minor percentage, ~6%, were found over endosomes (Figure 6C). Notably, the plasma membrane and dense lysosomes (Figures 6A and 7B) were devoid of VAMP4 label, indicating that VAMP4 does not reside in the endocytic pathway but recycles to the TGN. In the Golgi stack, VAMP4 resided primarily on the medial to *trans*-cisternae (Figure 6A). In the TGN, VAMP4 was found on both vesicular and tubular membranes, ~40% of which in double labeling also stained for clathrin (Table 1 and Figure 6B). Noteworthy, VAMP4 was found on ISGs, identified by the presence of a clathrin coat, but not on mature SGs (Figure 6B). A similar observation was previously made for syntaxin 6 in endocrine pancreatic and exocrine parotid cells (Klumperman *et al.*, 1998), and it was shown that syntaxin 6 exits ISGs via AP1- and clathrin-coated vesicles. The present observations suggest that VAMP4 also follows the clathrin-mediated pathway to exit TGN and ISGs in PC12 cells. Double labeling of VAMP4 and syntaxin 6 showed that these two SNARE proteins colocalize in the same TGN membranes (Figure 7B) (Bock *et al.*, 1997). The ER–Golgi intermediate compartment at the *cis* side of the Golgi was invariably devoid of VAMP4, whereas the SNARE protein rbet1 could be readily detected in these membranes (Figure 7A)(Hay *et al.*, 1998). Taken together, the overall distribution pattern of VAMP4 in PC12 cells is comparable with that previously described for syntaxin 6 (Bock *et al.*, 1997), with the exception that significant label of VAMP4 is found in the Golgi stack.

Detergent-extracted VAMP4 Forms a Stable Protein Complex

A key step in understanding the physiological function of a SNARE protein is the elucidation of the protein–protein interactions it participates in. Different SNARE proteins have been found to form stable complexes in detergent extracts (Sollner *et al.*, 1993b; Bock *et al.*, 1997; Hay *et al.*, 1997). To determine whether VAMP4 exists in a high-molecular-mass protein complex, rat brain membranes were solubilized with Triton X-100 and subsequently fractionated on a linear glycerol gradient. The migration of VAMP4 and other vesicle-trafficking proteins was then monitored by SDS-PAGE and Western blotting. As shown in Figure 8, VAMP4 was found in low-molecular-mass fractions <25 kDa; however, a substantial pool of VAMP4 migrated in higher-molecular-mass fractions with two peaks, one at ~43 kDa and another at ~160–180 kDa. As a comparison, we immunoblotted the fractions of the same velocity gradient for different SNARE proteins and for the VAMP-binding protein synaptophysin. VAMP2 peaked in fraction 6, corresponding to a molecular mass of 43 kDa. Coinciding with this, the majority of synaptophysin resided in the same fractions. Syntaxin 1 peaked at fractions 10 and 11, corresponding to a molecular mass of 140–160 kDa. Syntaxin 6 immunoreactivity was broadly distributed throughout the gradient, indicating that it might form a multiplicity of different complexes. These data demonstrate that VAMP4 is present in a large stable protein

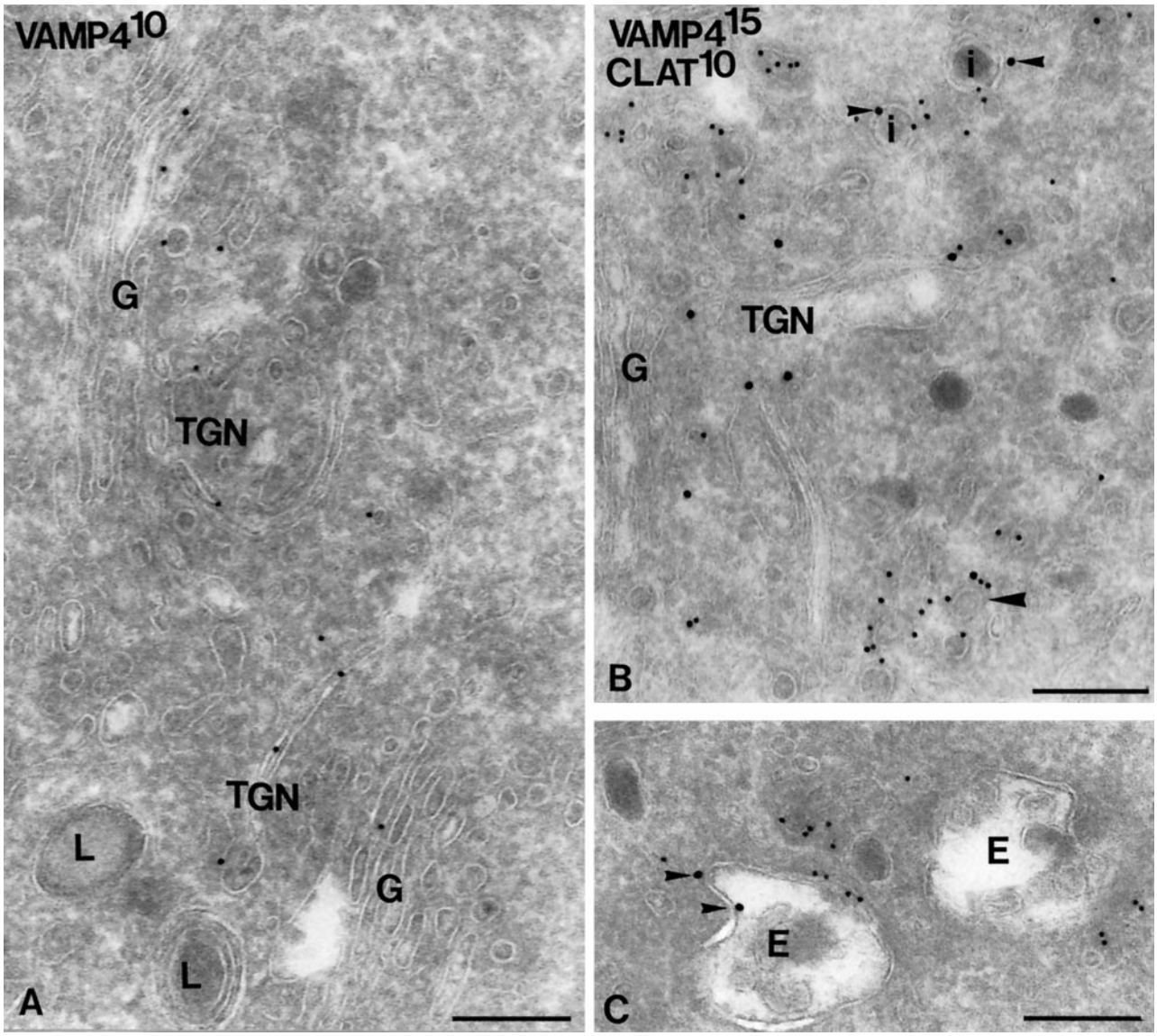

Figure 6. VAMP4 localizes to the Golgi apparatus and the TGN. (A) Double-immunogold labeling of VAMP4 (10-nm gold) and negative control antibody 3C9.H6 (15-nm gold). Only VAMP4-representing 10-nm gold particles are seen. VAMP4 predominantly localizes to the Golgi stack (G) and vesicular and tubular TGN membranes in close vicinity to the Golgi stack. Lysosomes (L) are negative. (B and C) Double-immunogold labeling of VAMP4 (15-nm gold) and clathrin (10-nm gold). VAMP4 is present on clathrin-coated vesicles in the TGN (large arrowhead in B). Additional VAMP4 labeling (indicated by small arrowheads) is present at the limiting membranes of clathrin-positive ISGs (I in B) and of endosomal vacuoles (E in C). SGs that do not stain for clathrin are also negative for VAMP4. Bars, 200 nm.

complex(es), perhaps representing a functional homologue of the synaptic 7S vesicle docking–fusion complex (Sollner *et al*., 1993a).

Purification and Characterization of Proteins Associated with VAMP4

To identify the individual members of the oligomeric VAMP4 protein complex(es), we carried out large-scale immunoprecipitations from rat brain membrane extracts using affinity-purified anti-VAMP4 antibodies. Immunoprecipitates were fractionated on an SDS-polyacrylamide gel, which was subsequently stained with Coomassie blue (Figure 9A). In addition to VAMP4 (p18), we found several other protein bands specific to immune precipitates. The coprecipitation of these bands was specific, because these associated proteins were not coprecipitated with control IgG. Seven abundant and specific protein bands were excised,

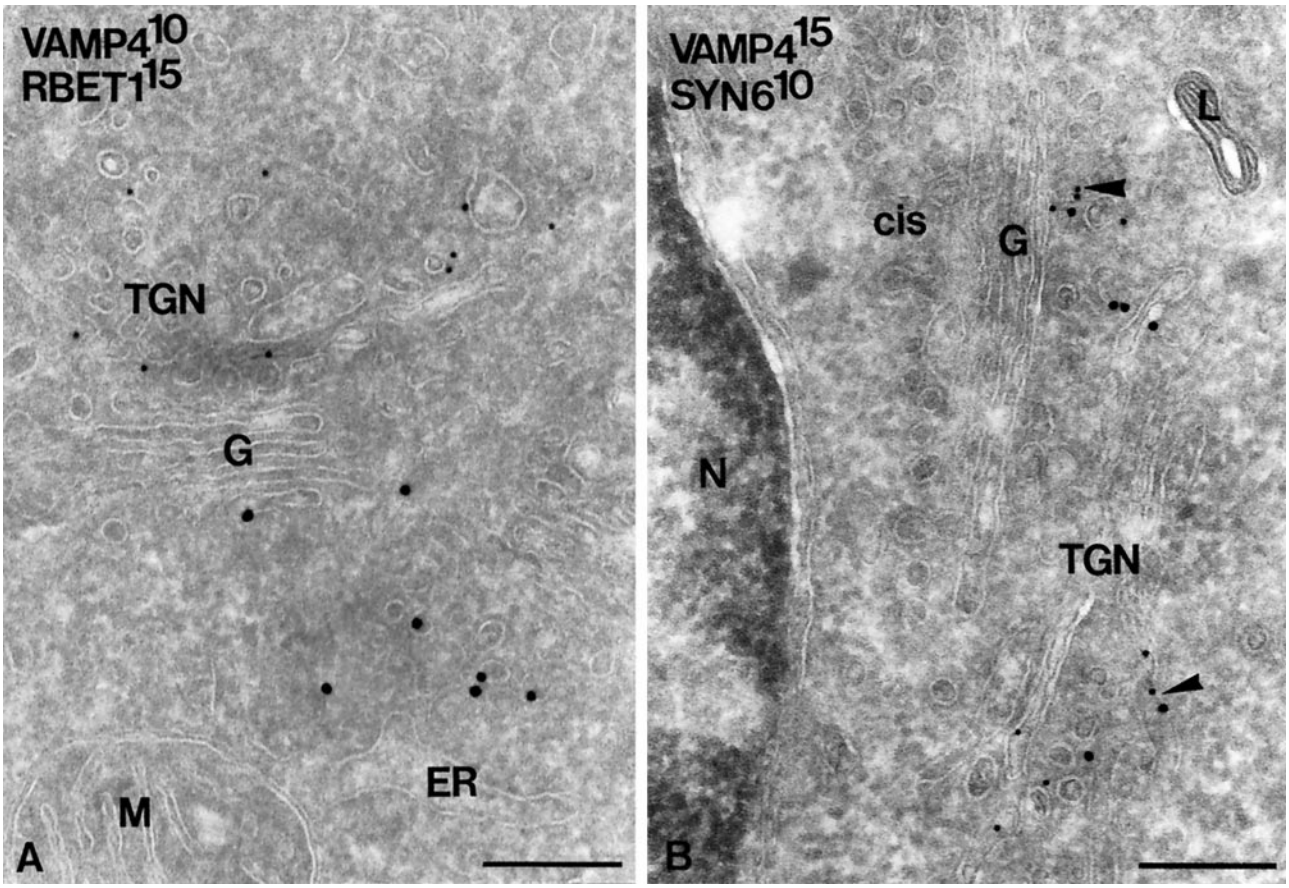

Figure 7. VAMP4 colocalizes with syntaxin 6. (A) Double-immunogold labeling of VAMP4 (10-nm gold) and rbet1 (15-nm gold). The two SNARE proteins clearly reside in distinct membranes at either side of the Golgi stack. (B) Double-immunogold labeling of VAMP4 (15-nm gold) and syntaxin 6 (10-nm gold) showing colocalization to the same TGN membranes (large arrowheads). The extensive ER–Golgi intermediate compartment at the *cis* side of the Golgi is devoid of both VAMP4 and syntaxin 6. L, lysosome. Bars, 200 nm.

digested with the protease lysC, and the resulting peptides were subjected to Edman sequence analysis (Table 2). Additional proof for the identity of these proteins was obtained by mass spectrometric analysis of the obtained peptides and/or by Western blot analysis.

The sequences obtained from bands p16 and p18 corresponded to a mixture of different VAMP proteins. In addition to VAMP4 (p18), we also obtained sequences from VAMP1/3 (p16 and p18). Because of the high sequence homology between VAMP1 and VAMP3, we were not able to distinguish between these two proteins (McMahon *et al.*, 1993). The presence of other VAMP proteins in the immunoprecipitate is surprising, because the affinity-purified anti-VAMP4 antibodies do not cross-react with other VAMP proteins, including the highly homologous isoforms (Figure 1A). However, this issue was potentially clarified when two additional coprecipitated proteins were identified. A major band (p40) was identified as synaptophysin, a protein previously shown to bind to

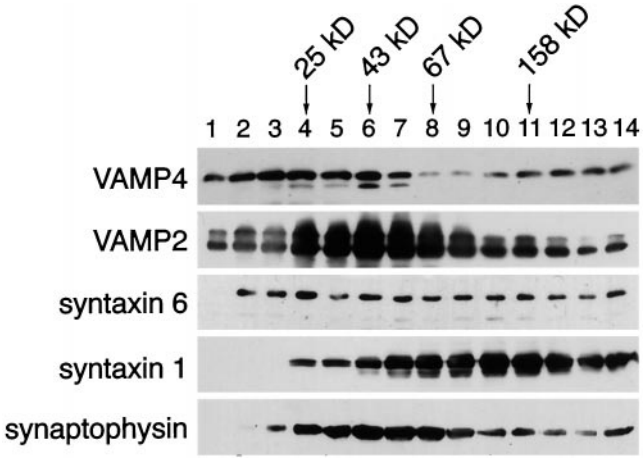

Figure 8. VAMP4 is a member of an ~50- and ~160-kDa protein complex. Rat brain membrane extract was fractionated by centrifugation through an 11–35% glycerol velocity gradient, and sequential fractions were analyzed by electrophoresis and immunobloting with antibodies against VAMP4, VAMP2, syntaxin 6, syntaxin 1, and synaptophysin. Arrows indicate the mobilities of marker proteins.

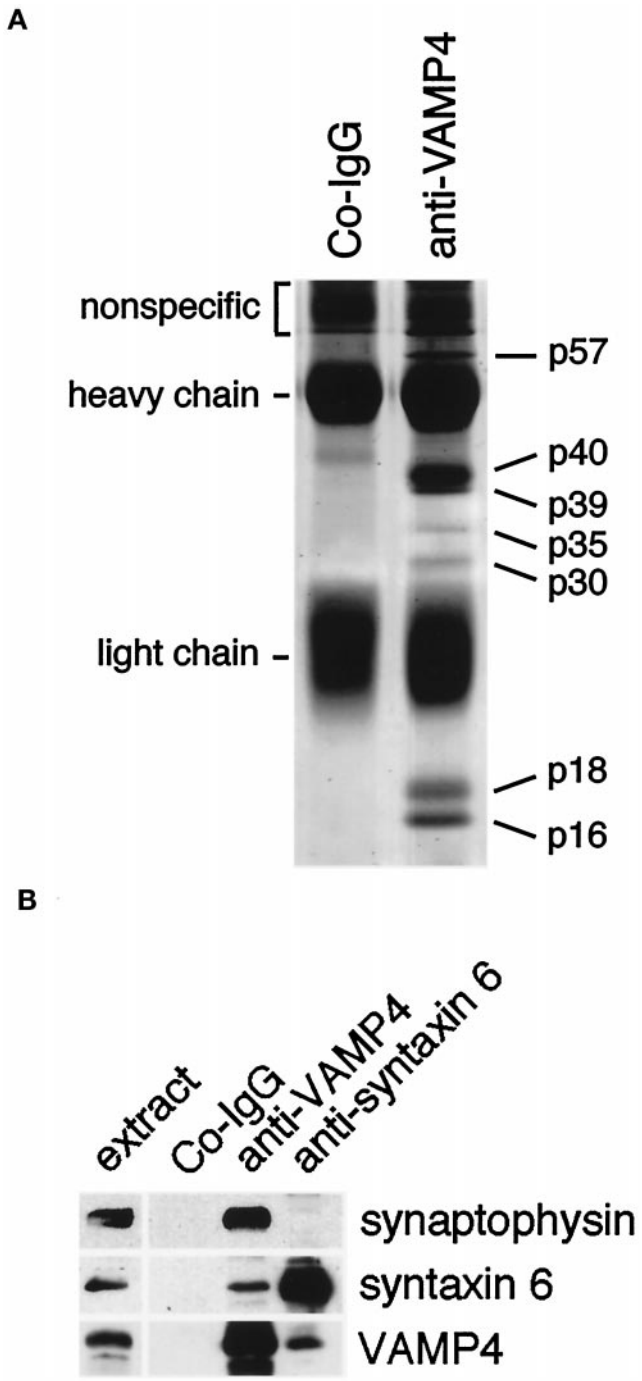

Figure 9. VAMP4 associates with at least six vesicle-trafficking proteins in two different protein complexes. (A) Crude membranes from rat brain were isolated and solubilized with 1% Triton X-100. The solubilized membranes were incubated with protein A-Sepharose beads loaded with either affinity-purified rabbit anti-VAMP4 antibodies or with nonspecific rabbit IgG. After the binding step the beads were washed, eluted with SDS protein sample dye, resolved by SDS-PAGE, and stained with Coomassie blue. The indicated bands were excised from the gel and subjected to internal amino acid sequencing (see Table 2). (B) Immunoprecipitations with control IgG, anti-VAMP4, and anti-syntaxin 6 antibodies were carried out as detailed in MATERIALS AND METHODS, and the resulting precipitates were analyzed by electrophoresis and immunoblotting. Labels along the top correspond to the antibodies used for immunoprecipitation, whereas labels along the right indicate the antibodies used for immunobloting. Note that synaptophysin is precipitated with anti-VAMP4 but not with anti-syntaxin 6 antibodies.

VAMP2 (Calakos and Scheller, 1994; Edelmann *et al.*, 1995). The sequences from the band p39 corresponded to peptide stretches present in physophillin/Ac39. Physophillin is a synaptic plasma membrane protein, which has been shown to bind to synaptophysin (Thomas and Betz, 1990; Carrion-Vazquez *et al.*, 1998). Thus, it seems likely that VAMP4 binds to synaptophysin, which in turn may also form a higher-order complex with physophilin. Furthermore, our results suggest that synaptophysin may be capable of forming complexes with more then one VAMP molecule at the time, thereby resulting in the observed indirect coprecipitation of VAMP4 and VAMP1/3. Alternatively, VAMP4 might form dimeric complexes with other VAMP molecules. Calakos and Scheller (1994) have shown that two distinct VAMP-immunoreactive complexes of 30 and 56 kDa are recovered after chemical cross-linking of detergent-solubilized rat brain homogenates. The 30-kDa complex most likely represents a dimer of two VAMP molecules.

VAMP1/2 has been shown to form a stable protein complex with syntaxin 1 and SNAP-25 (Sollner *et al.*, 1993a). It is therefore expected that VAMP4 might associate with one or more members of the syntaxin/SNAP-25 protein family to form an equivalent docking–fusion complex. Indeed, microsequencing and Western blot analysis identified p30 as syntaxin 6 (Bock *et al.*, 1996, 1997). This interaction is specific because other syntaxin molecules were not coprecipitated with VAMP4 (Fig. 9A). Although syntaxin 1 and other syntaxin molecules are highly expressed in brain, the immunoprecipitation did not yield sufficient quantities of these proteins to detect them by Coomassie blue staining. The interaction of VAMP4 with syntaxin 6 detected by coprecipitation is consistent with our indirect immunofluorescence and ultrastructural analysis, in which we localized both SNARE molecules to the same membranes of the TGN.

The peptide sequences from the 35-kDa protein band were identical to regions of αSNAP (Table 2). Bock *et al.* (1996) have shown that αSNAP binds syntaxin 6. αSNAP–SNARE complexes in turn can bind NSF, and NSF-dependent hydrolysis of ATP dissociates the complex, separating the individual SNARE molecules (Sollner *et al.*, 1993a).

The peptide sequence we obtained from p57 did not enable us to identify this coprecipitated protein (Table 2). Blast searches did not show any significant homology of p57 with any other protein in the databases. It

Table 2. Peptide sequences from VAMP4-associated proteins

Protein band (kDa)	Peptide sequences obtained	Identity (residues)
57	ELFLGHIQQK	
40	QPAPGDAYGDAGYGQGPGGYGPQDSYGPQGGYQ	Synaptophysin (238–270)
39	LFPHCG	Physophilin (240–245)
	TLEDRFFEHEVK	Physophilin (289–300)
35	VAGYAAQLEQYQK	αSNAP (168–180)
	FFSGLFG	αSNAP (27–33)
30	FNLDATELSIRK	Syntaxin 6 (78–89)
18	SESLSDNATAFSNRSK	VAMP4 (88–103)
	LSELDD	VAMP1/3 (62–67/47–52)
16	LSELDDRADALQ	VAMP1/3 (62–73/47–58)

The molecular masses of the protein bands are indicated as in Figure 8. Parentheses in the right column indicate amino acids corresponding to the peptide sequence obtained. The peptide sequence obtained from the 57-kDa protein did not show significant homology to any known protein.

is unlikely that p57 represents an additional member of the isolated SNARE complex, because SNARE proteins are typically not significantly higher in molecular mass than 35–40 kDa. One possibility is that p57 represents a cargo molecule that interacts with vesicle-trafficking molecules.

The oligomeric protein complex precipitated with anti-VAMP4 antibodies may not be a single homogeneous complex but is likely to represent two subcomplexes. Evidence for the existence of two distinct VAMP4-containing subcomplexes was obtained by fractionation of rat brain membrane extracts over glycerol velocity gradients (Figure 8) and by small-scale immunoprecipitation experiments with anti-VAMP4 and anti-syntaxin 6 antibodies (Figure 9B). Whereas anti-VAMP4 antibodies coprecipitated syntaxin 6 and synaptophysin, anti-syntaxin 6 immunoprecipitations yielded in the coisolation of VAMP4 but not of synaptophysin. Additionally, we were able to detect a direct interaction between recombinant VAMP4 and GST-syntaxin 6 in bead-binding experiments. Together, these data demonstrate that brain detergent extracts contain at least two distinguishable pools of VAMP4: one complexed with synaptophysin and physophilin and another complexed to syntaxin 6, i.e. a SNARE complex.

DISCUSSION

To better understand the organization of membrane compartments in mammalian cells, it is necessary to determine the precise subcellular localization and the pairing specificity of SNARE proteins. We previously identified VAMP4 as a novel member of the VAMP/synaptobrevin family and suggested its involvement in Golgi–TGN membrane trafficking based on the localization of transfected epitope-tagged protein (Advani *et al.*, 1998). In this report we present a detailed analysis of the subcellular distribution of endogenous VAMP4 and demonstrate the existence of VAMP4 in a SNARE complex containing syntaxin 6. Converging lines of evidence suggest that VAMP4 mediates a TGN vesicle-trafficking event, possibly from the TGN to endosomes.

Although the mammalian secretory pathway has been under intensive investigation, little is known about the SNARE machinery residing within the TGN, mediating trafficking events to various membrane compartments, including the recycling of MPRs between the TGN and endosomes. Syntaxin 6, which was identified by its homology to the endosomal SNARE Pep12p in yeast, has been shown to localize to tubovesicular membrane structures of the TGN (Bock *et al.*, 1996, 1997). Our ultrastructural studies demonstrated that VAMP4 shows striking colocalization with syntaxin 6 on tubular and vesicular TGN membrane structures. A significant pool (31% of the total label) of VAMP4 was found on clathrin-coated membranes, predominantly located in the TGN. Both the cation-dependent and -independent MPRs are also concentrated in clathrin-coated membranes and vesicles in the TGN (Klumperman *et al.*, 1993). A notable portion of the VAMP4 label was found on endosomes. Interestingly, the labeling of ultrathin cryosections of PC12 cells also revealed that a minor but significant pool of VAMP4 is present on ISGs. These organelles can be viewed as functional extensions of the TGN, where proteins that are not destined for regulated secretion are actively sorted out by a clathrin- and AP-1-dependent mechanism (Dittie *et al.*, 1996; Kuliawat *et al.*, 1997). Recently, syntaxin 6, in parallel with MPR and clathrin and AP-1, was found to be removed from maturing SGs in endocrine and exocrine pancreatic cells (Klumperman *et al.*, 1998). Most likely, VAMP4, together with syntaxin 6 and MPRs, is actively sorted out of maturing granules in secretory cells. This observation, together with the finding that

both VAMP4 and syntaxin 6 could not be detected on the plasma membrane, strongly argues against a role of these SNARE proteins in TGN-to-plasma membrane trafficking.

The colocalization of VAMP4 and syntaxin 6, observed by our light-level studies, provides an additional line of evidence for the TGN localization of VAMP4. It has been reported previously that treatment of cells with BFA causes redistribution of *cis*-, medial-, and *trans*-Golgi markers into the ER, whereas membranes of the TGN collapse toward the MTOC (Lippincott-Schwartz *et al.*, 1991; Reaves and Banting, 1992). A 15-min treatment of CHO cells with BFA was sufficient to relocalize virtually all of the VAMP4 immunoreactivity as well as syntaxin 6 to the area around the MTOC. Because VAMP4 does not behave like a protein of the Golgi stack upon treatment with BFA, but rather colocalizes with markers of the TGN–endosomal system, a post-Golgi localization of VAMP4 seems most likely. Although our EM studies revealed a minor pool of VAMP4 localized to stacks of the medial- and *trans*-Golgi, we did not observe that a detectable pool of VAMP4 redistributed to the intermediate compartment or ER upon BFA treatment. Most likely, this minor Golgi pool of VAMP4 could not be detected because of the limited sensitivity and resolution of our indirect immunomicroscopy studies. Alternatively, CHO cells in contrast to PC12 cells do not have a detectable Golgi pool of VAMP4. In cells treated with nocodazole, the VAMP4 staining is segregated from that of transferrin receptor but localized to the same vesicular structures as syntaxin 6. Therefore, these data, in conjunction with the EM immunogold labeling in PC12 cells, strongly suggest that VAMP4 is primarily associated with the TGN. The TGN localization could represent the end point or the starting point of the transport step mediated by VAMP4. One hint toward the answer of this question is the observation that a significant pool of VAMP4 is found on clathrin- and AP1-coated vesicles or clathrin-coated structures budding from the TGN. The differential incorporation of cargo into distinct coated buds at the TGN is believed to be an active process that is dependent on cytosol-oriented sorting signals. The dileucine motif LL as well as thyrosine-based signal have been identified as sorting signals for lysosomal delivery (Letourneur and Klausner, 1992; Kirchhausen *et al.*, 1997). VAMP4 contains such a dileucine motif at amino acids 25 and 26. This dileucine motif might be indeed sufficient to trigger the incorporation of VAMP4 into clathrin-coated vesicles destined for endosomes. In this scenario, the predominant TGN localization would represent the start point of the transport step mediated by VAMP4. Clathrin-coated vesicles would resemble transport intermediates in this transport step. VAMP4-positive noncoated vesicles might resemble a retrograde transport step in which VAMP4, perhaps together with MPRs, gets recycled back to domains of the TGN where VAMP4 resided before accumulating into clathrin-coated vesicles. Our observation that only 6% of the total VAMP4 label was found on endosomes argues for a rapid recycling of VAMP4 back to the TGN. It has been shown that MPRs enter and rapidly leave the endosomal–prelysosomal compartment, and therefore, at steady state most of the MPRs reside in the TGN (Klumperman *et al.*, 1993; Hirst *et al.*, 1998). Alternatively, the TGN could also be the end point of the VAMP4-mediated transport step. In this case, VAMP4 would be involved in the vesicular transport from an endosomal compartment back to the TGN, e.g., the targeting of MPR-containing vesicles back to the TGN. However, the presence of VAMP4 on clathrin-coated vesicles argues against this model, because this retrograde transport step seems not to use a clathrin coat (Draper *et al.*, 1990).

The tight colocalization of VAMP4 and syntaxin 6 observed by indirect immunofluorescence and immunogold EM argues for a physical interaction of the two SNARE molecules. Indeed, immunoprecipitation experiments with anti-VAMP4 antibodies demonstrated that a significant pool of VAMP4 is bound to syntaxin 6. In detergent extracts most of the VAMP4 protein was found in a complex with synaptophysin, physophilin, and VAMP1/3. The neuronal VAMP isoforms 1 and 2 have been shown to bind with high affinity to synaptophysin, whereas a nonneuronal isoform of VAMP (VAMP3/cellubrevin) displayed a lower but still significant affinity for synaptophysin (Calakos and Scheller, 1994; Edelmann *et al.*, 1995). Because of the abundance of synaptophysin in brain membrane lysates, it is not surprising that a large pool of the VAMP4 protein associates with synaptophysin. However, indirect immunofluorescence microscopy on embryonic hippocampal cultures shows little overlap between VAMP4 and synaptophysin. Thus, the physiological significance of this interaction remains to be determined. The interaction of synaptophysin with neuronal VAMP excludes the integration of syntaxin 1a into the same complex (Edelmann *et al.*, 1995; Calakos and Scheller, 1996). Likewise, we found that anti-syntaxin 6 antibodies coprecipitate VAMP4 but not synaptophysin. We therefore conclude that in brain membrane detergent extracts VAMP4 is present in two distinguishable pools: one complexed to synaptophysin, which simultaneously binds to physophilin and to additional VAMP isoforms; and another complexed to syntaxin 6 in a SNARE complex, with no overlap between them. Previous studies have shown that syntaxin 6 is also capable of interacting with VAMP3/cellubrevin and/or VAMP2 (Bock *et al.*, 1997). This finding might indicate that despite its tight colocalization with VAMP4, syntaxin 6 might mediate more than one trafficking step. This is not a unique

finding; e.g., yeast Vti1p has been found to bind to more than one syntaxin isoform (Holthuis *et al.*, 1998).

In summary, we have presented several lines of evidence that VAMP4 mediates a TGN vesicle-trafficking event, most likely transport from the TGN to late endosomes. Our localization data, together with the identification of syntaxin 6 as a binding partner for VAMP4, now provide an indispensable framework to direct future studies of these SNARE molecules.

ACKNOWLEDGMENTS

We thank V. Oorschot for the preparation of ultrathin cryosections and M. Niekerk, T. van Rijin, and R. Scriwaneck (all four from University of Utrecht) for handling the electron micrographs. We thank R. Winant of the Stanford Protein and Nucleic Acid facility for amino acid sequencing.

REFERENCES

Advani, R.J., Bae, H.R., Bock, J.B., Chao, D.S., Doung, Y.C., Prekeris, R., Yoo, J.S., and Scheller, R.H. (1998). Seven novel mammalian SNARE proteins localize to distinct membrane compartments. J. Biol. Chem. *273*, 10317–10324.

Banker, G.A., and Cowan, W.M. (1977). Rat hippocampal neurons in dispersed cell culture. Brain Res. *126*, 397–442.

Bennett, M.K., and Scheller, R.H. (1994). A molecular description of synaptic vesicle membrane trafficking. Annu. Rev. Biochem. *63*, 63–100.

Bock, J.B., Klumperman, J., Davanger, S., and Scheller, R.H. (1997). Syntaxin 6 functions in trans-Golgi network vesicle trafficking. Mol. Biol. Cell *8*, 1261–1271.

Bock, J.B., Lin, R.C., and Scheller, R.H. (1996). A new syntaxin family member implicated in targeting of intracellular transport vesicles. J. Biol. Chem. *271*, 17961–17965.

Calakos, N., and Scheller, R.H. (1994). Vesicle-associated membrane protein and synaptophysin are associated on the synaptic vesicle. J. Biol. Chem. *269*, 24534–24537.

Calakos, N., and Scheller, R.H. (1996). Synaptic vesicle biogenesis, docking, and fusion: a molecular description. Physiol. Rev. *76*, 1–29.

Carrion-Vazquez, M., Fernandez, A.M., Chowen, J., and Nieto-Sampedro, M. (1998). Brain Ac39/physophilin: cloning, coexpression and colocalization with synaptophysin. Eur. J. Neurosci. *10*, 1153–1166.

Dittie, A.S., Hajibagheri, N., and Tooze, S.A. (1996). The AP-1 adaptor complex binds to immature secretory granules from PC12 cells, and is regulated by ADP-ribosylation factor. J. Cell Biol. *132*, 523–536.

Draper, R.K., Goda, Y., Brodsky, F.M., and Pfeffer, S.R. (1990). Antibodies to clathrin inhibit endocytosis but not recycling to the trans Golgi network in vitro. Science *248*, 1539–1541.

Edelmann, L., Hanson, P.I., Chapman, E.R., and Jahn, R. (1995). Synaptobrevin binding to synaptophysin: a potential mechanism for controlling the exocytotic fusion machine. EMBO J. *14*, 224–231.

Galli, T., Chilcote, T., Mundigl, O., Binz, T., Niemann, H., and De Camilli, P. (1994). Tetanus toxin-mediated cleavage of cellubrevin impairs exocytosis of transferrin receptor-containing vesicles in CHO cells. J. Cell Biol. *125*, 1015–1024.

Hanson, P.I., Heuser, J.E., and Jahn, R. (1997a). Neurotransmitter release—four years of SNARE complexes. Curr. Opin. Neurobiol. *7*, 310–315.

Hanson, P.I., Roth, R., Morisaki, H., Jahn, R., and Heuser, J.E. (1997b). Structure and conformational changes in NSF and its membrane receptor complexes visualized by quick-freeze/deep-etch electron microscopy. Cell *90*, 523–535.

Hay, J.C., Chao, D.S., Kuo, C.S., and Scheller, R.H. (1997). Protein interactions regulating vesicle transport between the endoplasmic reticulum and Golgi apparatus in mammalian cells. Cell *89*, 149–158.

Hay, J.C., Hirling, H., and Scheller, R.H. (1996). Mammalian vesicle trafficking proteins of the endoplasmic reticulum and Golgi apparatus. J. Biol. Chem. *271*, 5671–5679.

Hay, J.C., Klumperman, J., Oorschot, V., Steegmaier, M., Kuo, C.S., and Scheller, R.H. (1998). Localization, dynamics, and protein interactions reveal distinct roles for ER and Golgi SNAREs. J. Cell Biol. *141*, 1489–1502.

Hay, J.C., and Scheller, R.H. (1997). SNAREs and NSF in targeted membrane fusion. Curr. Opin. Cell Biol. *9*, 505–512.

Hirst, J., Futter, C.E., and Hopkins, C.R. (1998). The kinetics of mannose 6-phosphate receptor trafficking in the endocytic pathway in HEp-2 cells: the receptor enters and rapidly leaves multivesicular endosomes without accumulating in a prelysosomal compartment. Mol. Biol. Cell *9*, 809–816.

Holthuis, J.C., Nichols, B.J., Dhruvakumar, S., and Pelham, H.R. (1998). Two syntaxin homologues in the TGN/endosomal system of yeast. EMBO J. *17*, 113–126.

Hsu, S.C., Ting, A.E., Hazuka, C.D., Davanger, S., Kenny, J.W., Kee, Y., and Scheller, R.H. (1996). The mammalian brain rsec6/8 complex. Neuron *17*, 1209–1219.

Inoue, A., Obata, K., and Akagawa, K. (1992). Cloning and sequence analysis of cDNA for a neuronal cell membrane antigen, HPC-1. J. Biol. Chem. *267*, 10613–10619.

Kirchhausen, T., Bonifacino, J.S., and Riezman, H. (1997). Linking cargo to vesicle formation: receptor tail interactions with coat proteins. Curr. Opin. Cell Biol. *9*, 488–495.

Klausner, R.D., Donaldson, J.G., and Lippincott-Schwartz, J. (1992). Brefeldin A: insights into the control of membrane traffic and organelle structure. J. Cell Biol. *116*, 1071–1080.

Klumperman, J., Hille, A., Veenendaal, T., Oorschot, V., Stoorvogel, W., von Figura, K., and Geuze, H.J. (1993). Differences in the endosomal distributions of the two mannose 6-phosphate receptors. J. Cell Biol. *121*, 997–1010.

Klumperman, J., Kuliawat, R., Griffith, J.M., Geuze, H.J., and Arvan, P. (1998). Mannose 6-phosphate receptors are sorted from immature secretory granules via adaptor protein AP-1, clathrin, and syntaxin 6-positive vesicles. J. Cell Biol. *141*, 359–371.

Kornfeld, S. (1992). Structure and function of the mannose 6-phosphate/insulin-like growth factor II receptors. Annu. Rev. Biochem. *61*, 307–330.

Kuliawat, R., Klumperman, J., Ludwig, T., and Arvan, P. (1997). Differential sorting of lysosomal enzymes out of the regulated secretory pathway in pancreatic beta-cells. J. Cell Biol. *137*, 595–608.

Letourneur, F., and Klausner, R.D. (1992). A novel di-leucine motif and a tyrosine-based motif independently mediate lysosomal targeting and endocytosis of CD3 chains. Cell *69*, 1143–1157.

Liou, W., Geuze, H.J., and Slot, J.W. (1996). Improving structural integrity of cryosections for immunogold labeling. Histochem. Cell Biol. *106*, 41–58.

Lippincott-Schwartz, J., Donaldson, J.G., Schweizer, A., Berger, E.G., Hauri, H.P., Yuan, L.C., and Klausner, R.D. (1990). Microtubule-dependent retrograde transport of proteins into the ER in the presence of brefeldin A suggests an ER recycling pathway. Cell *60*, 821–836.

Lippincott-Schwartz, J., Yuan, L., Tipper, C., Amherdt, M., Orci, L., and Klausner, R.D. (1991). Brefeldin A's effects on endosomes, lysosomes, and the TGN suggest a general mechanism for regulating organelle structure and membrane traffic. Cell *67*, 601–616.

Matteoni, R., and Kreis, T.E. (1987). Translocation and clustering of endosomes and lysosomes depends on microtubules. J. Cell Biol. *105*, 1253–1265.

McMahon, H.T., Ushkaryov, Y.A., Edelmann, L., Link, E., Binz, T., Niemann, H., Jahn, R., and Sudhof, T.C. (1993). Cellubrevin is a ubiquitous tetanus-toxin substrate homologous to a putative synaptic vesicle fusion protein [see comments]. Nature *364*, 346–349.

McNew, J.A., Sogaard, M., Lampen, N.M., Machida, S., Ye, R.R., Lacomis, L., Tempst, P., Rothman, J.E., and Sollner, T.H. (1997). Ykt6p, a prenylated SNARE essential for endoplasmic reticulum-Golgi transport. J. Biol. Chem. *272*, 17776–17783.

Mellman, I., and Simons, K. (1992). The Golgi complex: in vitro veritas? Cell *68*, 829–840.

Nakamura, N., Lowe, M., Levine, T.P., Rabouille, C., and Warren, G. (1997). The vesicle docking protein p115 binds GM130, a *cis*-Golgi matrix protein, in a mitotically regulated manner. Cell *89*, 445–455.

Orci, L., Ravazzola, M., Amherdt, M., Madsen, O., Vassalli, J.D., and Perrelet, A. (1985). Direct identification of prohormone conversion site in insulin-secreting cells. Cell *42*, 671–681.

Orci, L., Tagaya, M., Amherdt, M., Perrelet, A., Donaldson, J.G., Lippincott-Schwartz, J., Klausner, R.D., and Rothman, J.E. (1991). Brefeldin A, a drug that blocks secretion, prevents the assembly of non-clathrin-coated buds on Golgi cisternae. Cell *64*, 1183–1195.

Paek, I., Orci, L., Ravazzola, M., Erdjument-Bromage, H., Amherdt, M., Tempst, P., Sollner, T.H., and Rothman, J.E. (1997). ERS-24, a mammalian v-SNARE implicated in vesicle traffic between the ER and the Golgi. J. Cell Biol. *137*, 1017–1028.

Palade, G. (1975). Intracellular aspects of the process of protein synthesis. Science *189*, 347–358.

Pevsner, J., Hsu, S.C., Braun, J.E., Calakos, N., Ting, A.E., Bennett, M.K., and Scheller, R.H. (1994). Specificity and regulation of a synaptic vesicle docking complex. Neuron *13*, 353–361.

Poirier, M.A., Xiao, W., Macosko, J.C., Chan, C., Shin, Y.-K., and Bennet, M.K. (1998). The synaptic SNARE complex is a parallel four-stranded helical bundle. Nat. Struct. Biol. *5*, 765–769.

Reaves, B., and Banting, G. (1992). Perturbation of the morphology of the trans-Golgi network following Brefeldin A treatment: redistribution of a TGN-specific integral membrane protein, TGN38. J. Cell Biol. *116*, 85–94.

Rothman, J.E., and Wieland, F.T. (1996). Protein sorting by transport vesicles. Science *272*, 227–234.

Schekman, R., and Orci, L. (1996). Coat proteins and vesicle budding. Science *271*, 1526–1533.

Scheller, R.H. (1995). Membrane trafficking in the presynaptic nerve terminal. Neuron *14*, 893–897.

Slot, J.W., Geuze, H.J., Gigengack, S., Lienhard, G.E., and James, D.E. (1991). Immuno-localization of the insulin regulatable glucose transporter in brown adipose tissue of the rat. J. Cell Biol. *113*, 123–135.

Sollner, T., Bennett, M.K., Whiteheart, S.W., Scheller, R.H., and Rothman, J.E. (1993a). A protein assembly-disassembly pathway in vitro that may correspond to sequential steps of synaptic vesicle docking, activation, and fusion. Cell *75*, 409–418.

Sollner, T., Whiteheart, S.W., Brunner, M., Erdjument-Bromage, H., Geromanos, S., Tempst, P., and Rothman, J.E. (1993b). SNAP receptors implicated in vesicle targeting and fusion [see comments]. Nature *362*, 318–324.

Steegmaier, M., Yang, B., Yoo, J.S., Huang, B., Shen, M., Yu, S., Luo, Y., and Scheller, R.H. (1998). Three novel proteins of the syntaxin/SNAP-25 family. J. Biol. Chem. *274*, 34171–34179.

Sudhof, T.C. (1995). The synaptic vesicle cycle: a cascade of protein-protein interactions. Nature *375*, 645–653.

Sutton, R.B., Fasshauer, D., Jahn, R., and Brunger, A.T. (1998). Crystal structure of a SNARE complex involved in synaptic exocytosis at 2.4 A resolution [see comments]. Nature *395*, 347–353.

Thomas, L., and Betz, H. (1990). Synaptophysin binds to physophilin, a putative synaptic plasma membrane protein. J. Cell Biol. *111*, 2041–2052.

Tooze, J., and Tooze, S.A. (1986). Clathrin-coated vesicular transport of secretory proteins during the formation of ACTH-containing secretory granules in AtT20 cells. J. Cell Biol. *103*, 839–850.

Traub, L.M., and Kornfeld, S. (1997). The trans-Golgi network: a late secretory sorting station. Curr. Opin. Cell Biol. *39*, 527–533.

Turner, J.R., and Tartakoff, A.M. (1989). The response of the Golgi complex to microtubule alterations: the roles of metabolic energy and membrane traffic in Golgi complex organization. J. Cell Biol. *109*, 2081–2088.

Waters, M.G., Clary, D.O., and Rothman, J.E. (1992). A novel 115-kDa peripheral membrane protein is required for intercisternal transport in the Golgi stack. J. Cell Biol. *118*, 1015–1026.

Weber, T., Zemelman, B.V., McNew, J.A., Westermann, B., Gmachl, M., Parlati, F., Sollner, T.H., and Rothman, J.E. (1998). SNAREpins: minimal machinery for membrane fusion. Cell *92*, 759–772.

Wong, S.H., Zhang, T., Xu, Y., Subramaniam, V.N., Griffiths, G., and Hong, W. (1998). Endobrevin, a novel synaptobrevin/VAMP-like protein preferentially associated with the early endosome. Mol. Biol. Cell *9*, 1549–1563.

Zen, K., Notarfrancesco, K., Oorschot, V., Slot, J.W., Fisher, A.B., and Shuman, H. (1998). Generation and characterization of monoclonal antibodies to alveolar type II cell lamellar body membrane. Am. J. Physiol. *275*, L172–L183.

Zeng, Q., Subramaniam, V.N., Wong, S.H., Tang, B.L., Parton, R.G., Rea, S., James, D.E., and Hong, W. (1998). A novel synaptobrevin/VAMP homologous protein (VAMP5) is increased during in vitro myogenesis and present in the plasma membrane. Mol. Biol. Cell *9*, 2423–2437.